Article

SMMR
STATISTICAL METHODS IN MEDICAL RESEARCH

Functional joint models for chronic kidney disease in kidney transplant recipients

Statistical Methods in Medical Research
0(0) 1–12

DOI: 10.1177/09622802211009265
journals.sagepub.com/home/smm
SAGE

Jianghu (James) Dong[1,2], Jiguo Cao[3], Jagbir Gill[4], Clifford Miles[2] and Troy Plumb[2]

Abstract

This functional joint model paper is motivated by a chronic kidney disease study post kidney transplantation. The available kidney organ is a scarce resource because millions of end-stage renal patients are on the waiting list for kidney transplantation. The life of the transplanted kidney can be extended if the progression of the chronic kidney disease stage can be slowed, and so a major research question is how to extend the transplanted kidney life to maximize the usage of the scarce organ resource. The glomerular filtration rate is the best test to monitor the progression of the kidney function, and it is a continuous longitudinal outcome with repeated measures. The patient's survival status is characterized by time-to-event outcomes including kidney transplant failure, death with kidney function, and death without kidney function. Few studies have been carried out to simultaneously investigate these multiple clinical outcomes in chronic kidney disease stage patients based on a joint model. Therefore, this paper proposes a new functional joint model from this clinical chronic kidney disease study. The proposed joint models include a longitudinal sub-model with a flexible basis function for subject-level trajectories and a competing-risks sub-model for multiple time-to event outcomes. The different association structures can be accomplished through a time-dependent function of shared random effects from the longitudinal process or the whole longitudinal history in the competing-risks sub-model. The proposed joint model that utilizes basis function and competing-risks sub-model is an extension of the standard linear joint models. The application results from the proposed joint model can supply some useful clinical references for chronic kidney disease study post kidney transplantation.

Keywords

Competing-risks survival, basis function, random effects, joint models, CKD

1 Background and introduction

Kidney transplantation is the preferred therapy for kidney failure, but progressive loss of renal function over time after transplant is a significant problem. Estimated glomerular filtration rate (GFR) is a common bio-marker used in the monitoring of chronic kidney disease (CKD), but relatively, few studies have modeled GFR in CKD after kidney transplant. For example, one study[1] looked at the effect of the baseline CKD stage at 12 months and the slope of eGFR by comparing transplant patients with the native-kidney CKD, but there were only nine transplant patients in stage 4 and no patients in stage 5. Other studies[2,3] assumed the longitudinal GFR to be a linear

[1]Department of Biostatistics, University of Nebraska Medical Center, NE, USA
[2]Division of Nephrology, University of Nebraska Medical Center, NE, USA
[3]Department of Statistics and Actuarial Science, Simon Fraser University, Burnaby, Canada
[4]Department of Medicine, University of British Columbia, BC, Canada

Corresponding author:
Jianghu Dong, Department of Biostatistics, University of Nebraska Medical Center, NE, USA.
Email: jianghu.dong@unmc.edu

trajectory. Another study[4] looked at the effect of CKD stage at 12 months on the slope of GFR, where there was a substantial number of patients in stage 4 and only few in stage 5. Last, another study[5] had very few patients with eGFR less than $30\,\mathrm{ml/min/1.73\,m^2}$ and did not look at determinants of GFR trajectory. These studies that were plagued by the low number of transplant recipients with advanced CKD ($\mathrm{GFR} < 30\,\mathrm{ml/min/1.73\,m^2}$) or failure did not allow us to investigate nonlinear patterns of GFR trajectories.

It is important to describe patterns of GFR over time in CKD and develop models to predict disease progression to alert patients and providers to the need for preventive health interventions. In particular, the identification of individual dynamic patterns of trajectory, such as non-linear, non-progression, or rapid progression, with corresponding time-to-event associations, would be useful in the care of kidney transplant recipients. Comprehensive predictive models could be used to identify and test novel biomarkers or select patients that may benefit from alternative treatment strategies. We sought to develop a suitable joint model that could describe the individual dynamic trajectory of longitudinal progression of eGFR, in conjunction with corresponding associated time-to-event outcomes.

In many existing joint models for longitudinal and time-to-event data, it is assumed that individual longitudinal trajectories are characterized by a linear model with random intercepts and random time slopes over time. However, individual longitudinal trajectories need not be bound by a simple linear model. Brown et al.[6] developed a flexible Bayesian B-spline model for the longitudinal process that allowed for nonlinear trajectories in the proposed joint model. They applied their joint model to a dataset, where AIDS or death in patients are events, and the serial assessments of HIV viral load and CD4 counts are the longitudinal bio-markers. Rizopoulos and Ghosh[7] likewise proposed a Bayesian semi-parametric multivariate joint model by including a cubic spline-based approach in order to flexibly capture the possibly nonlinear shapes of the subject-specific trajectory. The study[8] has developed a joint model with the B-splines based on fractional polynomials. One limitation of the aforementioned joint models is focus on one time-to-event outcome. Therefore, alternative joint models with the competing-risk sub-model were developed for multiple outcomes, such as Elashoff et al.[9] and Hickey et al.,[10] where the joint distribution of two latent variables from the longitudinal sub-model and the competing-risk sub-model was constructed. In this proposed joint model, a flexible B-spline basis function was used to fit the subject longitudinal process, while the competing-risk sub-model was used to fit multiple possible time-to-event outcomes. Our proposed sub-survival model includes a spline form of integral or derivative of the B-spline function in the cumulative hazard. This is different from the paper by Kim et al.,[11] which used the coefficient of time-varying covariates in the longitudinal submodel as the latent factor linking the survival submodel.

There are several advantages for this study. First, one of the main contributions is that it is the first of its kind to develop functional joint model of CKD progression in kidney transplant recipients. It is useful for clinical practice to identify the potential risk factors for chronic kidney disease. We find that the non-linear GFR trajectories were significantly related to time-to-event outcomes from our proposed joint models. The linear decline does not apply to a large number of CKD patients, and it can cause a bias by assuming GFR to be a linear trajectory. It is also interesting to see that young patients are more likely to have kidney transplant failures before patient death compared with old patients. Second, the proposed joint model includes an individual B-spline basis function in the longitudinal sub-model and a competing-risk sub-model, which allows us to combine the dynamic longitudinal bio-marker with multiple time-to-event outcomes simultaneously. The proposed functional joint model can also explore the different association between the longitudinal trajectory and the time-to-event processes. The different association structures between the longitudinal and multiple time-to-event outcomes can be flexibly accommodated through a time-dependent function of shared random effects and the longitudinal procession. The rest of this article is organized as follows. The proposed joint models are introduced in Section 2. We present the estimation method for the joint model in Section 3. Section 4 demonstrates the application of our joint model in the transplantation clinical data. Section 5 presents the results of a simulation study. Conclusion and discussion are given in Section 6.

2 Joint model

The proposed functional joint models are given in the framework of multivariate joint models for the longitudinal and time-to-event outcomes. Let $Y_i(t_{ij})$ be a repeated continuous measured outcome at times t_{ij} for the ith subject, where $i = 1, \ldots, n$, $j = 1, \ldots, n_i$ and n_i is the number of repeated measurements for the ith subject. For example, the longitudinal outcome $Y_i(t_{ij})$ is the repeated measurements of GFR at different time points in the application example of transplant clinical data. Let T_i be the ith subject's survival time to the event of interest or censoring

time. Let (T_i, Δ_i) denote the competing risk data on the subjects, where $\Delta_i = 0$ indicating a censored event and $\Delta_i = d$ that showing this subject fails from the dth type of time-to events ($d = 1, \ldots, g$). Let $\boldsymbol{Z}_i = [Z_{i1}, \ldots, Z_{iP}]^T$ be the observed co-variate for the ith subject. We propose the following joint model

$$\begin{cases} Y_i(t) = \boldsymbol{\alpha}^T \boldsymbol{Z}_i + m_i(t, b_i) + \epsilon_i, i = 1, \ldots, n, \\ \lambda_d(t|\boldsymbol{Z}_i, \mathcal{M}(\boldsymbol{b}_i, m_i(t, \boldsymbol{b_i}))) = \lambda_{d,0}(t)\exp\{\boldsymbol{\beta_d}^T \boldsymbol{Z}_i + \boldsymbol{\gamma}_d^T \mathcal{M}(\boldsymbol{b}_i, m_i(t, \boldsymbol{b_i}))\} \end{cases} \tag{1}$$

The first equation in Model (1) is the longitudinal sub-model for repeated measurement outcome $Y_i(t_{ij})$, where $\boldsymbol{\alpha} = (\alpha_1, \ldots, \alpha_P)^T$ is a vector of coefficients for the fixed effects of $\boldsymbol{Z}_i = [Z_{i1}, \ldots, Z_{iP}]^T$ and $m_i(t, \boldsymbol{b_i}) = a_0 + b_{i0} + \sum_{k=1}^{K}(a_k + b_{ik})B_k(t) = (\boldsymbol{a} + \boldsymbol{b}_i)^T \boldsymbol{B}(t)$, where $\boldsymbol{a} = (a_0, a_1, \ldots, a_K)^T$ is a coefficient vector that represents the population-level longitudinal trajectories, $\boldsymbol{b}_i = (b_{i0}, b_{i1}, \ldots, b_{iK})^T$ is a vector of the random effects that characterize the individual trajectory, and $\boldsymbol{B}(t) = \{1, B_1(t), \ldots, B_K(t)\}$ is a vector of basis function of t, such as the B-spline basis. The vector of measurement errors $\epsilon_i = (\epsilon_{i1}, \ldots, \epsilon_{in_i})$ is assumed to be multivariate normal distributed with the mean 0 and variance-covariance matrix $\sigma^2 \boldsymbol{I}_n$.

The second equation in Model (1) is a competing-risks survival model. The hazard function $\lambda_d(t|\boldsymbol{Z}_i, \mathcal{M}_i(t))$ is the cause-specific hazard rate of the cumulative incidence function $F_d(t|\boldsymbol{Z}_i, \mathcal{M}_i(t))$ for the dth competing risk. The coefficient $\boldsymbol{\gamma}_d$ is a vector of association parameters between the longitudinal process and the survival process. The association structure function $\mathcal{M}_i(\boldsymbol{b}_i, m_i(t, \boldsymbol{b_i}))$ is dependent on the random effects $\boldsymbol{b}_i$ and the longitudinal process $m_i(t, \boldsymbol{b_i})$. This function can accomplish several different association structures between the longitudinal sub-model and the survival sub-model. If $\mathcal{M}(\boldsymbol{b}_i, m_i(t, \boldsymbol{b_i})) = \int_0^t m(s)ds$, then $\mathcal{M}_i(\boldsymbol{b}_i, m_i(t, \boldsymbol{b_i}))$ is the cumulative effects of $m_i(t, \boldsymbol{b_i})$. If $\mathcal{M}(\boldsymbol{b}_i, m_i(t, \boldsymbol{b_i})) = [m_i(t, \boldsymbol{b_i}), m_i'(t, \boldsymbol{b_i})]$, then the joint model in which the survival risk depends on both the current true value of the trajectory $m_i(t, \boldsymbol{b_i})$ and the slope of trajectory $m_i'(t, \boldsymbol{b_i})$ at t, such as one of joint models in the application section. If $\mathcal{M}(\boldsymbol{b}_i, m_i(t, \boldsymbol{b_i})) = \boldsymbol{b}_i$, then the joint model is called a shared random effect joint model, where the joint model only considers the random effects of the longitudinal sub-model. For example, a shared random effects joint model with an accelerated failure time sub-model for kidney and pancreas transplant patients was developed by Dong et al.[12] The advantage for that joint model is that it supplies an easy interpretation for the coefficients when a simple random-intercepts and random-slopes structure is assumed for the longitudinal sub-model.

3 Method

After specifying the proposed joint model in Section 2, we give the joint likelihood function in Section 3.1, and the algorithm is presented in Section 3.2.

3.1 The joint likelihood function

We construct the joint likelihood function in the general joint likelihood construction frame. The longitudinal and the time-to-event processes are assumed to be independent given the random effects vector $\boldsymbol{b_i}$ from the true longitudinal process $m_i(t, \boldsymbol{b_i})$ or the true process $m_i(t, \boldsymbol{b_i})$. The process $m_i(t, \boldsymbol{b_i})$ is dependent on the random effect vector $\boldsymbol{b_i}$ because the basis function $\boldsymbol{B}(t)$ is known. The function $\mathcal{M}_i(\boldsymbol{b}_i, m_i(t, \boldsymbol{b_i}))$ in the competing-risks sub-model is only dependent on the random effect vector $\boldsymbol{b_i}$. Therefore, the joint probability is given as follows without considering the fixed covariates $\boldsymbol{Z}_i$ for easy notation

$$f(T_i, \Delta_i, \boldsymbol{Y_i}|\boldsymbol{b_i}, \boldsymbol{\Theta}) = f(T_i, \Delta_i|\boldsymbol{\theta}_t, \boldsymbol{b_i})f(\boldsymbol{Y_i}|\boldsymbol{\theta}_y, \boldsymbol{b_i}) \tag{2}$$

where

$$f(\boldsymbol{Y_i}|\boldsymbol{\theta}_y, \boldsymbol{b_i}) = \prod_{k=1}^{K} f(\boldsymbol{Y_{ik}}|\boldsymbol{\theta}_y, \boldsymbol{b_{ik}})$$

where

$$f(\boldsymbol{Y_{ik}}|\boldsymbol{\theta_y}, \boldsymbol{b_{ik}}) = \prod_{j=1}^{n_{ik}} f(Y_{ij,k}|\boldsymbol{b_{ik}})$$

The parameter vector $\boldsymbol{\Theta}^T = (\boldsymbol{\theta}_t^T, \boldsymbol{\theta}_y^T, \boldsymbol{\theta}_{\boldsymbol{b}}^T)$ in equation (2) is the full parameter vector that needs to be estimated. The parameter vector $\boldsymbol{\theta}_t$ is the parameter for the event time outcome, $\boldsymbol{\theta}_y$ is the parameter for the longitudinal outcomes, and $\boldsymbol{\theta_b}$ is the parameter of the random-effects covariance matrix. Under these assumptions, the overall likelihood function based on the observed information is given by

$$L(T_i, \Delta_i, \boldsymbol{Y_i}, \boldsymbol{Z}_i, \boldsymbol{\theta}) = \prod_{i=1}^{n} \int f(T_i, \Delta_I|\boldsymbol{Z}_i, \boldsymbol{\theta}_t, \boldsymbol{b_i}) f(\boldsymbol{y_i}|\boldsymbol{Z}_i, \boldsymbol{\theta}_y, \boldsymbol{b_i}) f(\boldsymbol{b_i}, \boldsymbol{\theta}_b) d\boldsymbol{b_i} \tag{3}$$

where the conditional survival density function is

$$\begin{aligned} f(T_i, \Delta_i|\boldsymbol{Z}_i, \boldsymbol{\theta}_t, \boldsymbol{b}_i) = & \prod_{d=1}^{g} \lambda_d(t|\boldsymbol{Z}_i, \mathcal{M}(\boldsymbol{b}_i, m_i(t, \boldsymbol{b_i})))^{I(\Delta_i = d)} \\ & \times \exp\left[-\int_0^{T_i} \left\{ \sum_{d=1}^{g} \lambda_d(t|\boldsymbol{Z}_i, \mathcal{M}(\boldsymbol{b}_i, m_i(t, \boldsymbol{b_i}))) \right\} \mathrm{d}t \right] \end{aligned} \tag{4}$$

The function $f(Y_i|\boldsymbol{Z}_i, \boldsymbol{a}, \boldsymbol{b}_i, \boldsymbol{\alpha}, \sigma^2)$ is the density function of Normal$(\boldsymbol{\alpha}^T\mathbf{Z} + m_i(t, \boldsymbol{b_i}), \sigma^2)$ and the longitudinal process $m_i(t, \boldsymbol{b_i}) = (\boldsymbol{a} + \boldsymbol{b}_i)^T \boldsymbol{B}(t)$ as specified in Section 2. The distribution of the random effect $f(\boldsymbol{b}_i)$ is assumed to a normal distribution with the density function of Normal$(0, \mathbf{B})$. The score function can be expressed as in the following after the log-likelihood function given in the formula (3)

$$\begin{aligned} S(\boldsymbol{\theta}) &= \sum_{I=1}^{n} \frac{\partial}{\partial \boldsymbol{\theta}^T} \log \int f(T_i, \Delta_i \boldsymbol{Z}_i, |\boldsymbol{\theta}_t, \boldsymbol{b_i}) f(\boldsymbol{Y_i}|\boldsymbol{Z}_i, \boldsymbol{\theta}_y, \boldsymbol{b_i}) f(\boldsymbol{b_i}, \boldsymbol{\theta}_b) \mathrm{d}\boldsymbol{b_i} \\ &= \sum_{I=1}^{n} \int \frac{\partial}{\partial \boldsymbol{\theta}} \log[f(T_i, \Delta_i|\boldsymbol{Z}_i, \boldsymbol{\theta}_t, \boldsymbol{b_i}) f(\boldsymbol{Y_i}|\boldsymbol{Z}_i, \boldsymbol{\theta}_y, \boldsymbol{b_i}) f(\boldsymbol{b_i}, \boldsymbol{\theta}_b)] \\ &\quad \times f(\boldsymbol{b_i}|T_i, \Delta_i, \boldsymbol{Y_i}, \boldsymbol{Z}_i, \boldsymbol{\Theta}) \mathrm{d}\boldsymbol{b_i} \end{aligned} \tag{5}$$

From equation (5), the score function can be expressed as the expected value of the complete data score function with respect to the posterior distribution of the random effects $\boldsymbol{b_i}$ with $f(\boldsymbol{b_i}|T_i, \Delta_i, \boldsymbol{Y_i}, \boldsymbol{Z}_i, \boldsymbol{\Theta})$. The parameters $\boldsymbol{\alpha}$, a, $\boldsymbol{\beta}$, and $\boldsymbol{\gamma}$ can be estimated via maximizing the joint likelihood in equation (3). We propose to estimate the parameters by maximizing the joint likelihood function through the EM-algorithm because a vector of latent variables $\boldsymbol{b_i}$ exists in the joint likelihood function. The expectation of the joint likelihood function does not have a closed form when we integrate the latent feathers $\boldsymbol{b_i}$, so the Monte Carlo EM-algorithm is developed in Section 3.2.

3.2 Monte Carlo EM-algorithm

We propose to estimate the parameters in the joint model (1) by using the Monte Carlo EM-algorithm.[13] The EM-algorithm is an iterative procedure with two steps: the expectation (E) step and the maximization (M) step. If the integral in the E step is difficult to compute, the Monte Carlo method can be used to approximate the conditional expectation. After the E-step, the parameters can be estimated by locating the maximum of $l(\Theta)$ over all possible values of Θ. We often do not have a closed-form expression for each parameter from the gradient of the log-likelihood function with respect to the parameters. In this case, several algorithms are available to find the maximum of $l(\Theta)$ such as the Newton–Raphson method,[14] the Laplace transformation method,[15,16] or the Bayesian method.[17]

3.2.1. E-step

The expectation of the log-likelihood function can be expressed in the following

$$\begin{aligned} Q(\boldsymbol{\Theta}|\boldsymbol{\Theta}^{(t)}) &= E[l(\boldsymbol{\Theta}|T,\Delta,\boldsymbol{Y},\boldsymbol{Z})|\boldsymbol{\Theta}^{(t)}] \\ &= \sum_{i=1}^{n}\int [\log f(T_i,\Delta_i|\boldsymbol{b_i},\boldsymbol{Z_i},\boldsymbol{\theta}_t) + \sum_{j=1}^{n_i}\log f(Y_{ij}|\boldsymbol{b_i},\boldsymbol{Z_i},\boldsymbol{\theta}_y) \\ &\quad + \log f(\boldsymbol{b_i}|0,\mathbf{B})] f(\boldsymbol{b_i}|\boldsymbol{Y_i},\boldsymbol{Z_i},\boldsymbol{\Theta}^{(t)}) d\boldsymbol{b_i} \end{aligned} \tag{6}$$

It is difficult to obtain the integration of the log-likelihood function. We choose the Monte Carlo method to approximate the integration in equation (6). The tth iteration of the E-step can be modified by replacing $Q(\Theta|\Theta^{(t)})$ with a Monte Carlo estimate obtained as follows:

- Draw a sample $\boldsymbol{b_i}^{(I)},\ldots,\boldsymbol{b_i}^{(N)}$ from $f(\boldsymbol{b_i}|\mathbf{Z}_i,\boldsymbol{Y_i}(t),\boldsymbol{\Theta}^{(t)})$ based on the current approximation $\boldsymbol{\Theta}^{(t)}$, and compute the normalized weights $w_i^{(s)} \approx f(T_i,\Delta_i|\boldsymbol{b_i}^{(s)},\mathbf{Z}_i,\boldsymbol{\Theta}^{(t)})$.
- Calculate $\hat{Q}(\boldsymbol{\Theta}|\Theta^{(t)}) = \sum_{i=1}^{n}\sum_{s=1}^{N} l_i^{(s)}(\boldsymbol{\Theta}|T_i,\Delta_i,\mathbf{Z}_i,\boldsymbol{Y_i}(t),\boldsymbol{\Theta}^{(t)})$, where

$$l_i^{(s)} = \log f(T_i,\Delta_i|\boldsymbol{b_i}^{(s)},\boldsymbol{Z_i},\boldsymbol{\Theta}^{(t)}) + \sum_{j=1}^{n_i}\log f(Y_{ij}|\boldsymbol{b_i}^{(s)},\boldsymbol{Z_i},\boldsymbol{\Theta}^{(t)}) + \log f(\boldsymbol{b_i}^{(s)}|\boldsymbol{\Theta}^{(t)})$$

3.2.2. M-step

After computing the expectation for the random effect $\boldsymbol{b_i}$ in the log-likelihood function in equation (6), we also need to integrate the cumulative hazard function

$$\exp\left[-\int_0^{T_i}\left\{\sum_{d=1}^{g}\lambda_d(t|\mathbf{Z}_i,\mathcal{M}(\boldsymbol{b_i}^{(s)},m_i(t,\boldsymbol{b_i}^{(s)})))\right\}\mathrm{d}t\right]$$

in the density function $f(T_i,\Delta_i|\boldsymbol{b_i}^{(s)},\boldsymbol{Z_i},\boldsymbol{\Theta}^{(t)})$ in equation (4). These cumulative hazard functions do not have closed-form solutions. Therefore, a numerical integration approach is required. Here, we use the Gauss–Kronrod quadrature formula[18] for the integration approach as follows

$$\exp\left[-\int_0^{T_i}\phi(t)dt\right] \approx \exp\left[-\sum_{q=1}^{Q}\omega_q\phi(t_q)\right]$$

where $\phi(t_q) = \sum_{d=1}^{g}\lambda_d(t_q|\mathbf{Z}_i,\mathcal{M}(\boldsymbol{b_i}^{(s)},m_i(t_q,\boldsymbol{b_i}^{(s)})))$, ω_q is the quadrature weight, and t_q is the quadrature point to evaluate the function $\phi(t)$. After that, M-step estimates each parameter of $\boldsymbol{\Theta}$ by solving the derivative equations when they are equal to zero. We have obtained the estimate for the parameters $\hat{\boldsymbol{\alpha}}$, $\hat{\mathbf{B}}$, and $\hat{\sigma^2}$. The baseline hazard function $\hat{\lambda}_d(t)$ can be implemented by the step function. The last parameter to estimate is $\boldsymbol{\beta}$ and $\boldsymbol{\gamma}$

$$\boldsymbol{\Theta}^{(t+1)} = \mathrm{argmax}_\theta\, Q(\boldsymbol{\Theta}|\boldsymbol{\Theta}^{(t)})$$

The estimate for $\boldsymbol{\gamma}$ and $\boldsymbol{\beta}$ has no closed-form. So, we use the one-step Newton–Raphson approach to get it updated for the parameters $\boldsymbol{\gamma}^{t+1}$ and $\boldsymbol{\beta}^{t+1}$ in the M-step. We can repeat the E-step and M-step until all parameters converge at $\hat{\Theta}$. The convergence criterion for MCEM in the numerical study is

$$\max\left\{\frac{|\boldsymbol{\Theta}^t - \boldsymbol{\Theta}^{(t-1)}|}{|\boldsymbol{\Theta}| + \epsilon_2|} < \epsilon_1\right\}$$

where we set $\epsilon_2 = 0.002$ and $\epsilon_1 = 0.001$. The standard error of each estimated parameter of $\boldsymbol{\Theta}$ is computed using the bootstrap method.[19] We calculate the P-value by assuming that the ratio of the estimated coefficient over the standard error approximately follows a standard normal distribution.

4 Application results

4.1 Data cohort

A total of 1589 kidney-transplanted recipients were included in the application of the proposed models from the Canadian Organ Replacement Register data. The study time period was from 1 January 2001 to 31 December 2010. Patients with loss graft function or death during the first year were excluded. The last followed-up date was 31 December 2016 so that patients had at least five years of followed-up time. A total of 837 (53%) patients had at least one measurement of GFR $\leq 35\,\mathrm{ml/min/1.73\,m^2}$, and 752 patients (47%) did not have GFR $\leq 35\,\mathrm{ml/min/1.73\,m^2}$ post transplant. Among the 837 patients, 593 (71%) patients' kidney function had progressed to CKD stage 4 or 5, which was defined by the following conditions of patient GFR values. First, the index GFR date (time 0) is the 1st GFR $\leq 35\,\mathrm{ml/min/1.73\,m^2}$ after 365 days post-transplant. Second, the qualify window was set from the 75th day to the 105th day after the index GFR date. During the qualify window, all GFR post the index date had to stay below $35\,\mathrm{ml/min/1.73\,m^2}$. Otherwise, we did not count this patient as CKD 4/5 stage if the GFR values recovered to the above $35\,\mathrm{ml/min/1.73\,m^2}$. We find that the mean (SD) of the time range between the index date of GFR and the date of qualifying GFR was 88 (10) days.

Characteristics of kidney recipients were summarized by CKD 4/5 stage in Table 1. From Table 1, patients with a higher peak PRA were more likely to have a CKD 4/5 disease, for example, recipients with peak PRA 80 100

Table 1. Characteristics summary of kidney recipients by CKD stage.

	All patients	CKD stage 4/5	No CKD 4/5	
Variables	$N = 1589$	$N = 593$	$N = 996$	P value
Mean (SD) of age	48 (13)	48 (14)	49 (13)	0.422
Age 18–39	26	27	26	
Age 40–59	49	46	50	
Age $\geq$ 60	25	27	24	
Male (%)	61	59	62	0.340
Race (%)				0.065
White	63	65	61	
Oriental Asian	16	15	16	
South Asian	14	14	15	
Others	7	6	6	
PPRA (%)				<0.005
0	55	42	62	
1–19	25	25	25	
20–79	11	13	10	
80–100	9	20	3	
Transplant era (%)				0.145
2001–2004	34	35	34	
2005–2010	66	65	66	
Prior transplant (%)	11	24	3	<0.005
Baseline GFR at one year	59 (18)	48 (18)	66 (14)	<0.005
Mean (SD) of donor age	44 (14)	47 (14)	41 (14)	<0.005
Donor type (%)				0.054
DD	50	51	49	
LD	50	49	51	
Summary of time to event outcomes				
Graft failure	263 (17%)	247 (42%)	16 (2%)	<0.005
Death without kidney function	157 (10%)	98 (17%)	61 (6%)	<0.005
Death with kidney function	116 (7%)	102 (17%)	14 (2%)	<0.005
Mean(SD) of the study time (years)	9.72 (3.20)	9.64 (3.40)	9.76 (3.10)	<0.005

accounted for 80% CKD 4/5 vs 20% no CKD 4/5. Patients who had a previous kidney transplant were more likely to have CKD 4/5 disease, such as accounting for 82% CKD 4/5 versus 18% no CKD 4/5. Patients with the lower level baseline GFR at one year were more likely to have a CKD 4/5 event. Compared with the recipients transplanted with a deceased donor, kidney recipients with a living donor were less likely to have a CKD 4/5 event. CKD 4/5 patients significantly increased the probability of graft failure and death. For example, 42% of CKD 4/5 patients have graft failure compared with 2% non CKD 4/5 patients. We find that the occurrence of a CKD 4/5 event was a red alert for graft failure, which was one of the primary interesting findings. It is interesting to see that 116 (7%) patients had died with graft function. We are focusing on CKD 4/5 patients. Patients can have different trajectories to reach CKD stage 4/5. After patients reached CKD stage 4/5, patients also had different trajectories to reach the time-to-event outcomes like kidney failure. We investigated the association of GFR trajectory and time-to-event outcomes including kidney failure and death based on the proposed joint model, and the model results are presented in Section 4.3.

4.2 Specified joint model

We apply the proposed joint models to this clinical chronic kidney disease study. The flexible B-spline basis function is used to fit the longitudinal process of GFR trajectory in the proposed joint model. For the survival process in the joint model, we consider the competing-risk models for multiple time-to-event outcomes including graft failure and death.

Three different association structure functions of $\mathcal{M}_i(\boldsymbol{b}_i, m_i(t, b_i))$ are constructed in this application example. Each of these three joint models displays a different association between the longitudinal process and the survival process. First, if let $\mathcal{M}(\boldsymbol{b}_i, m_i(t, \boldsymbol{b_i})) = m_i(t, \boldsymbol{b_i})$, the joint model is specified as follows

$$\begin{cases} Y_i(t) = \boldsymbol{\alpha}^T \boldsymbol{Z}_i + a_0 + b_{i0} + \sum_{k=1}^{3} (a_k + b_{ik}) B_k(t) + \epsilon_i, \\ \lambda_d(t|\boldsymbol{Z}_i, \mathcal{M}(\boldsymbol{b}_i, m_i(t, \boldsymbol{b_i}))) = \lambda_{d,0}(t) \exp\{\boldsymbol{\beta_d}^T \boldsymbol{Z}_i + \gamma_{d1} m_i(t, \boldsymbol{b_i})\} \end{cases} \tag{7}$$

where $B_k(t)$ denotes the cubic B-spline basis function, and $i = 1, \ldots, n$. Second, let $\mathcal{M}(\boldsymbol{b}_i, m_i(t, \boldsymbol{b_i})) = \int_0^t m(s, \boldsymbol{b_i}) ds$, then $\mathcal{M}_i(\boldsymbol{b}_i, m_i(t, \boldsymbol{b_i}))$ is the cumulative effects of $m_i(t, \boldsymbol{b_i})$. The joint model is specified as follows

$$\begin{cases} Y_i(t) = \boldsymbol{\alpha}^T \boldsymbol{Z}_i + a_0 + b_{i0} + \sum_{k=1}^{3} (a_k + b_{ik}) B_k(t) + \epsilon_i, \\ \lambda_d(t|\boldsymbol{Z}_i, \mathcal{M}(\boldsymbol{b}_i, m_i(t, \boldsymbol{b_i}))) = \lambda_{d,0}(t) \exp\{\boldsymbol{\beta_d}^T \boldsymbol{Z}_i + \gamma_{d1} \int m_i(s, \boldsymbol{b_i}) ds\} \end{cases} \tag{8}$$

Third, if let $\mathcal{M}(\boldsymbol{b}_i, m_i(t, \boldsymbol{b_i})) = [m_i(t, \boldsymbol{b_i}), m_i'(t, \boldsymbol{b})]$, then the survival risk sub-model of the joint model depends on both the current true value of the trajectory $m_i(t, \boldsymbol{b_i})$ and the slope of trajectory $m_i'(t, \boldsymbol{b_i})$ at the t. The joint model is specified

$$\begin{cases} Y_i(t) = \boldsymbol{\alpha}^T \boldsymbol{Z}_i + a_0 + b_{i0} + \sum_{k=1}^{3} (a_k + b_{ik}) B_k(t) + \epsilon_i, \\ \lambda_d(t|\boldsymbol{Z}_i, \mathcal{M}(\boldsymbol{b}_i, m_i(t, \boldsymbol{b_i}))) = \lambda_{d,0}(t) \exp\{\boldsymbol{\beta_d}^T \boldsymbol{Z}_i + \gamma_{d1} m_i(t, \boldsymbol{b_i}) + \gamma_{d2} m_i'(t, \boldsymbol{b_i})\} \end{cases} \tag{9}$$

The number of degrees of freedom in the longitudinal model is determined from AIC and BIC. Also, another two separate joint models with separate Cox sub-model are chosen to fit this clinical data for the purpose of comparison. One is for GFR and death, and the other is for GFR and graft failure by censoring death. These two separate joint models allow us to see the resulting difference from modeling one time-to-event outcome without

considering the other time-to-event outcome through comparing with the proposed joint models with the competing-risk survival model

$$\begin{cases} Y_i(t) = \boldsymbol{\alpha}^T \boldsymbol{Z}_i + a_0 + b_{i0} + \sum_{k=1}^{3} (a_k + b_{ik}) B_k(t) + \epsilon_i, \\ \lambda_1(t|\boldsymbol{Z}_i, \mathcal{M}(\boldsymbol{b}_i, m_i(t, \boldsymbol{b_i}))) = \lambda_0(t) \exp\{\boldsymbol{\beta_1}^T \boldsymbol{Z}_i + \gamma_{11} m_i(t, \boldsymbol{b_i})\}, \\ \lambda_2(t|\boldsymbol{Z}_i, \mathcal{M}(\boldsymbol{b}_i, m_i(t, \boldsymbol{b_i}))) = \lambda_0(t) \exp\{\boldsymbol{\beta_2}^T \boldsymbol{Z}_i + \gamma_{21} m_i(t, \boldsymbol{b_i})\}. \end{cases} \tag{10}$$

4.3 Model result

Table 2 shows the coefficients of the co-variates from the longitudinal process in functional Joint Models (7), (8), (9), and (10). All coefficients of the B-spline are statistically significant in the longitudinal process. As mentioned in the introduction, the conventional proposal in the literature to assume that the change of the GFR curves is primarily linear. The significance of the B-spline base functions indicates that the linear assumption might result in an incomplete depiction of the variation within the GFR curves as well as its effects. Such a linear assumption may lead to biased findings in the literature.

Table 3 shows the coefficients of the co-variates from the competing-risks sub-survival models in functional Joint Models (7), (8), (9), and (10). It is an interesting finding that younger patients are more likely to have kidney transplant failures before patient death. Relative to the age group from 18 to 35, the coefficients of patients who are in age groups from 40 to 59 and more than 60 are negative. In other words, old patients are more likely to have a death event before they have kidney failure, and so some patients died with good kidney function. Compared with the elderly patients, the graft life of younger patients tends to be shorter. Among distinct association structure functions $\mathcal{M}_i(\boldsymbol{b}_i, m_i(t, b_i))$ in functional Joint Models (7), (8), (9), and (10), we find that the functional Joint Model (9) with $m(t)$ and $m(t)'$ is the best model based on AIC and BIC. The parameter vector $\boldsymbol{\gamma}_1$ measures the strength of the association between the current value of the longitudinal marker and the risk for the time-to-event, and parameter $\boldsymbol{\gamma}_2$ measures the strength of the association between the dynamic change value of the longitudinal marker and the risk for the time-to-event. From Table 3, both $\boldsymbol{\gamma}_1$ and $\boldsymbol{\gamma}_2$ in Model (9) are statistically significant with P-values less than 0.05.

5 Simulation study

In this section, the simulation study is implemented to access the finite-sample performance of the best proposed functional joint model with $m(t)$ and $m(t)'$ from the application example. We assume 500 patients who have been

Table 2. Longitudinal sub-model results in joint models.

	Model (7)	Model (8)	Model (9)	Model (10)
	Coef. (SE)	Coef. (SE)	Coef. (SE)	Coef. (SE)
Age	–0.10 (0.05)*	–0.10 (0.05)*	–0.09 (0.05)*	–0.08 (0.01)*
Female	0.74 (0.34)*	0.73 (0.34)*	0.75 (0.34)*	0.91 (0.21)*
Oriental Asian	5.04 (0.68)*	5.04 (0.68)*	5.08 (0.65)*	5.02 (0.16)*
South Asian	5.34 (0.23)*	5.35 (0.23)*	5.34 (0.23)*	5.14 (0.21)*
Others	1.18 (0.15)*	1.18 (0.15)*	1.19 (0.15)*	1.71 (0.15)*
PPRA 1–29	–0.98 (0.21)*	–0.98 (0.21)*	–0.98 (0.21)*	–0.87 (0.19)*
PPRA 30–100	–1.03 (0.23)*	–1.03 (0.23)*	–1.04 (0.23)*	–0.94 (0.24)*
Prior transplant	1.40 (0.19)*	1.38 (0.18)*	1.39 (0.19)*	1.37 (0.16)*
Donor age 40–59	–2.68 (0.16)*	–2.58 (0.16)*	–2.51 (0.16)*	–3.49 (0.13)*
Donor age $\geq$ 60	–8.47 (0.21)*	–7.97 (0.21)*	–8.54 (0.21)*	–10.75 (0.17)*
Living donor	3.32 (0.18)*	3.29 (0.29)*	3.43 (0.38)*	4.21 (0.12)*
a_0	39.97 (2.92)*	39.97 (2.92)*	40.14 (2.92)*	38.79 (1.36)*
a_1	–3.71 (0.72)*	–3.70 (0.70)*	–2.69 (0.70)*	–3.59 (0.59)*
a_2	–5.02 (0.81)*	–4.99 (0.80)*	–5.01 (0.81)*	–5.15 (0.48)*
a_3	–7.41 (0.99)*	–7.40 (0.99)*	–7.41 (0.99)*	–7.53 (0.42)*

*Denotes P value < 0.05.

Table 3. Competing risks sub-model results from joint models.

	Model (7)	Model (8)	Model (9)	Model (10)
	Coef. (SE)	Coef. (SE)	Coef. (SE)	Coef. (SE)
The graft failure primary event				
Age 40–59	–0.78 (0.18)*	–0.70 (0.18)*	–0.72 (0.18)*	0.38 (0.17)*
Age $\geq$ 60	–1.23 (0.17)*	–1.30 (0.17)*	–1.24 (0.17)*	0.82 (0.23)*
Female	–0.20 (0.11)*	–0.23 (0.11)*	–0.22 (0.12)*	–0.45 (0.15)*
Oriental Asian	0.53 (0.39)	0.53 (0.39)	0.53 (0.39)	0.51 (0.22)
South Asian	0.86 (0.52)	0.86 (0.52)	0.86 (0.52)	0.31 (0.24)
Others	0.75 (0.46)	0.78 (0.46)	0.75 (0.46)	0.79 (0.28)
PPRA 1–29	0.98 (0.20)*	1.08 (0.20)*	0.96 (0.19)*	0.76 (0.21)*
PPRA 30–100	1.03 (0.21)*	0.97 (0.21)*	1.01 (0.21)*	0.99 (0.19)*
Prior transplant	0.01 (0.18)	0.01 (0.18)	0.01 (0.18)	0.79 (0.20)
Living donor	–0.12 (0.08)*	–0.14 (0.08)*	–0.15 (0.08)*	–0.17 (0.10)*
Donor age 40–59	0.13 (0.32)	0.14 (0.32)	0.14 (0.32)	0.20 (0.21)
Donor age $\geq$ 60	0.17 (0.39)	0.14 (0.39)	0.15 (0.39)	0.32 (0.17)
γ_{11}	–0.10 (0.01)*	–0.10 (0.01)*	–0.09 (0.01)*	–0.17 (0.01)*
γ_{12}			–0.04 (0.01)*	
The death event				
Age 40–59	0.82 (0.20)*	0.75 (0.20)*	0.85 (0.20)*	1.15 (0.26)*
Age $\geq$ 60	1.47 (0.19)*	1.65 (0.19)*	1.57 (0.19)*	2.21 (0.28)*
Female	–0.47 (0.17)*	–0.43 (0.14)*	–0.39 (0.12)*	–0.58 (0.17)*
Oriental Asian	–0.52 (0.39)	–0.52 (0.39)	–0.52 (0.39)	–0.20 (0.24)
South Asian	–0.43 (0.41)	–0.44 (0.41)	–0.43 (0.41)	–0.16 (0.31)
Others	–0.82 (0.34)	–0.75 (0.34)	0.72 (0.34)	–0.74 (0.46)
PPRA 1–29	0.98 (0.23)	0.94 (0.21)	0.87 (0.18)	1.05 (0.20)
PPRA 30–100	1.03 (0.22)	0.93 (0.19)	1.04 (0.24)	0.78 (0.31)
Prior transplant	0.27 (0.18)	0.27 (0.18)	0.27 (0.18)	0.23 (0.25)
Donor age 40–59	0.06 (0.17)	0.08 (0.19)	0.07 (0.19)	0.05 (0.21)
Donor age $\geq$ 60	0.27 (0.30)	0.27 (0.31)	0.27 (0.23)	0.26 (0.26)
Living donor	0.03 (0.10)	0.05 (0.10)	0.04 (0.10)	–0.13 (0.17)
γ_{21}	–0.030 (0.01)*	–0.032 (0.01)*	–0.021 (0.01)*	–0.05 (0.01)*
γ_{22}			–0.008 (0.001)*	
Log likelihood	–166,220	–166,212	–166,201	–166,291
AIC	332,505	332,491	332,442	332,651
BIC	332,648	324,360	332,639	332,798

*Denotes P-value $<$ 0.05.

Table 4. Means, biases, and RMSEs of the parameter estimates for the joint model (11).

	The longitudinal submodel				The survival submodel			
Parameters	True	Mean	Bias	RMSE	True	Mean	Bias	RMSE
α_0	43.240	43.011	0.229	0.928				
α_1	–4.700	–4.655	–0.045	0.495				
α_2	–5.650	–5.569	–0.081	0.515				
α_3	–6.420	–6.328	–0.092	0.534				
γ_{11}					–0.090	–0.090	0.000	0.002
γ_{12}					–0.040	–0.041	0.001	0.003
γ_{21}					0.050	0.052	–0.002	0.006
γ_{22}					0.030	0.029	0.001	0.005

followed-up for a period of 15 years. The simulation procedure is repeated for 100 replicates. A multivariate mixed-effects model is chosen to simulate the longitudinal trajectories

$$\begin{cases} Y_i(t) = m_i(t, \boldsymbol{b}_i) + \epsilon_i, i = 1, \ldots, n \\ \lambda_d(t|\mathcal{M}_i(t, \boldsymbol{b}_i)) = \lambda_{d,0}(t)\exp\{\gamma_{d1} m_i(t, b_i) + \gamma_{d2} m_i'(t, b_i)\}, \quad d = 1, 2, \end{cases} \tag{11}$$

where the measurement error $\epsilon_i \sim$Normal(0, 1), $m_i(t, b_i) = a_0 + b_{i0} + (a_1 + b_{i1})B_1(t) + (a_2 + b_{i2})B_2(t) + (a_3 + b_{i3})B_3(t)$, and $\boldsymbol{b}_i \sim$Normal$(\boldsymbol{0}, \Sigma)$. We set $\alpha_0 = 43.24$, $\alpha_1 = -4.70$, $\alpha_2 = -5.65$, and $\alpha_3 = -6.42$. The closed-form integrals and derivative of the B-spline function was given in De Boor.[20] This can be implemented in the derivative functions dbs.() and ibs.() in R. Two internal knots were placed at three and six years in this

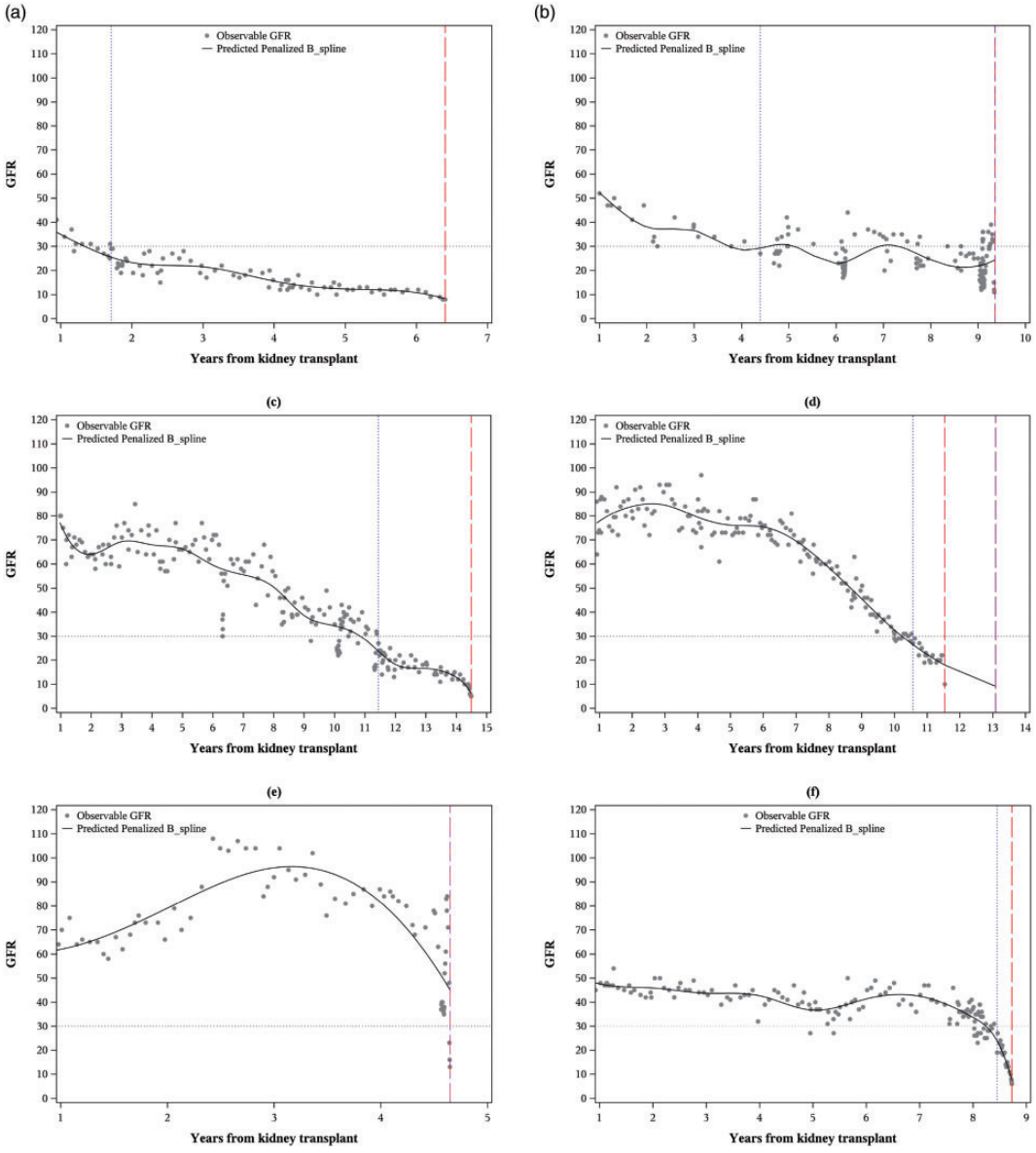

Figure 1. Observed GFR trajectory curves are in the dotted lines with various trajectory patterns. The predicted penalized B-splines are in the solid line. The dotted vertical line (blue) is the time that GFR reached CKD stage 4/5. The dashed vertical line (red) is the time of graft failure. The long-dashed (purple) vertical line is the time of death. Patients in the top panel ((a) and (b)) have flat GFR trends, and their kidney function was slowly moving to graft failure from CKD 4/5. Patients in the middle panels were decreasing much faster than the top panel ((a) and (b)). Patients in the bottom panel ((e) and (f)) were declining most rapidly and reached graft failure in a short time.

simulation, and boundary knots were set at 0.5 and 13 years. The scheduled measurement times of the repeated longitudinal outcome are set at the sequence year $(1, 2, \ldots, 15)$ for each subject, but there are no measurements available after death or censoring time. Both the baseline hazard function of the time to the primary event and the competing risk event are assumed to follow Weilbull distribution with the shape at 3.58. The hazard functions are specified in equation (11). Censoring times were simulated from a uniform distribution in the interval (0,15). Table 4 shows the parameter estimates, together with biases and root mean square errors (RMSEs). It shows that the means of the parameter estimates by the proposed method are close to their true values.

6 Conclusion and discussion

Here, we propose functional joint models including subject-level B-spline longitudinal sub-model and competing risk sub-model. We apply the proposed functional joint models to chronic kidney disease research for kidney-transplanted recipients. To the best of our knowledge, it is the first time to investigate chronic kidney disease in kidney-transplanted recipients post kidney transplantation based on functional joint models with a competing risks sub-model.

There are several findings in this paper. First, we find that recipients with high-peak PRA were more likely to have CKD 4 or 5 stage, patients who have had a previous kidney transplant were more likely to have CKD 4 or 5 stage, and patients with CKD 4 or 5 stage were more likely to have kidney failure. Second, the linear decline did not apply to a large number of CKD patients, and it can cause a bias by assuming GFR to be a linear trajectory. Third, the competing-risks survival sub-model can incorporate hazard ratios of multiple time-to-event outcomes. Although we can analyze two time-to event outcomes in two separate joint models, it may cause a bias through censoring one of multiple outcomes rather than joint modeling two time-to-events simultaneously. Furthermore, we find that the functional joint model (9) with $m(t)$ and $m(t)'$ is the best model from AIC and BIC among the proposed functional joint models (7), (8), (9), and (10) with distinct association structure functions $\mathcal{M}_i(\boldsymbol{b}_i, m_i(t, b_i))$ between the longitudinal and survival models.

The results from the proposed joint model provide at least two useful guidelines for the clinical practice. First, it confirmed that the non-linear GFR trajectories were significantly related to time-to-event outcomes. For example, patients with a non-progressive or slowly progressive trajectory at the beginning in the panel (e and f) of Figure 1 may have a clinical event, such as an acute kidney injury, which caused not only an abrupt drop of GFR but also a potential kidney failure. This descriptive result was consistent with the results from our proposed joint model (9). The dynamic slope of GFR trajectory $m(t)'$ in the joint model (9) was negatively correlated with graft failure, with a hazard ratio 95% CI (0.96 (0.94, 0.98)). This indicated that this patient was at more risk to have graft failure when GFR abruptly decreased. In addition, patients with lower GFR were more likely to have grafted loss because $m(t)$ in the joint model (9) was significantly negatively correlated with graft failure, with a hazard ratio 95% CI (0.91 (0.90, 0.93)). Second, it was very interesting to see that young patients were more likely to have kidney transplant failures before patient death as shown in the joint model (9). For example, compared with patients with age from 18 to 35, the hazard ratio (95% CI) of kidney failure in patients with age between 40 and 59 years old was 0.49 (0.34, 0.69), which was different from the hazard ratio (1.46 (1.05, 2.04)) from the joint model (10) by censoring death. Similarly, the hazard ratio (95% CI) of kidney failure in patients with age older 60 years old in the joint model (9) was 0.29 (0.21, 0.40), which was different from the hazard ratio (2.27 (1.45, 3.56)) from the joint model (10) by censoring death. The kidney life of young patients was shorter than the patient life time, while the kidney life of old patients was longer than the patient life time. Therefore, those younger patients with kidney failure need to have another kidney transplant; this is contrary to common knowledge and expectation. To make the best use of the scarce organ resource, it is worth investigating the cause of such a discrepancy, for example, possible differences in the quality of the donor's organ or biased preferences in assigning and allocating organ resources.

Declaration of conflicting interests

The author(s) declared no potential conflicts of interest with respect to the research, authorship, and/or publication of this article.

Funding

The author(s) received no financial support for the research, authorship, and/or publication of this article.

ORCID iDs

Jianghu (James) Dong https://orcid.org/0000-0001-6579-7442
Jiguo Cao https://orcid.org/0000-0001-7417-6330

References

1. Djamali A, Kendziorski C, Brazy PC, et al. Disease progression and outcomes in chronic kidney disease and renal transplantation. *Kidney Int* 2003; **64**: 1800–1807.
2. Gourishankar S, Hunsicker LG, Jhangri GS, et al. The stability of the glomerular filtration rate after renal transplantation is improving. *J Am Soc Nephrol* 2003; **14**: 2397–2394.
3. Gill JS, Tonelli M, Mix CH, et al. The change in allograft function among long-term kidney transplant recipients. *J Am Soc Nephrol* 2003; **64**: 1800–1807.
4. Marcén R, Morales JM, Fernández-Rodriguez A, et al. Long-term graft function changes in kidney transplant recipients. *Nephrol Dial Transpl* 2010; **9**: ii2–ii8.
5. Ferro CJ, Hodson J, Moore J, et al. Bayesian analysis of glomerular filtration rate trajectories in kidney transplant recipients: a pilot study *Transplantation* 2015; **99**: 533–539.
6. Brown ER, Ibrahim JG and DeGruttola V. A flexible B-spline model for multiple longitudinal biomarkers and survival. *Biometrics* 2005; **61**: 64–73.
7. Rizopoulos D and Ghosh P. A Bayesian semiparametric multivariate joint model for multiple longitudinal outcomes and a time-to-event. *Stat Med* 2011; **30**: 1366–1380.
8. Crowther MJ, Abrams KR and Lambert PC. Flexible parametric joint modelling of longitudinal and survival data. *Stat Med* 2012; **31**: 4456–4471.
9. Elashoff R, Li G and Li N. A joint model for longitudinal measurements and survival data in the presence of multiple failure types. *Biometrics* 2008; **164**: 762–771.
10. Hickey G, Philipson P, Jorgensen A, et al. A comparison of joint models for longitudinal and competing risks data, with application to an epilepsy drug randomized controlled trial. *J R Stat Soc* 2018; **181**: 1105–1123.
11. Kim S, Zeng D and Taylor J. Joint partially linear model for longitudinal data with informative drop-outs. *Biometrics* 2017; **73**: 72–82.
12. Dong J, Wang S, Wang L, et al. Joint modelling for organ transplantation outcomes for patients with diabetes and the end-stage renal disease. *Stat Method Med Res* 2019; **28**: 2724–2737.
13. Wei G and Tanner M. A Monte Carlo implementation of the EM algorithm and the poor man's data augmentation algorithms. *J Am Stat Assoc* 1990; **85**: 699–704.
14. Mordecai A. *Nonlinear programming: analysis and methods*. Mineola, NY: N.J. Dover Publishing, 2003.
15. Joe H. Accuracy of Laplace approximation for discrete response mixed models. *Comput Stat Data Anal* 2008; **52**: 5066–5074.
16. Rue H, Martino S and Chopin N. Approximate Bayesian inference for latent Gaussian models by using integrated nested Laplace approximations. *J R Stat Soc: Ser B* 2009; **71**: 319–392.
17. Luo S. A Bayesian approach to joint analysis of multivariate longitudinal data and parametric accelerated failure time. *Stat Med* 2004; **33**: 580–594.
18. Kahaner D, Moler C and Nash S. *Numerical methods and software*. Englewood Cliffs, NJ: Prentice-Hall, 1989.
19. Efron B and Tibshirani RJ. *An introduction to the bootstrap*. London, UK: CRC Press, 1994.
20. Boor D. *A practical guide to splines*. New York, NY: Springer-Verlag, 2007.